

Review

# The Advances and Applications of Characterization Technique for Exosomes: From Dynamic Light Scattering to Super-Resolution Imaging Technology

Shijia Wu <sup>1,†</sup>, Yalan Zhao <sup>1,†</sup>, Zitong Zhang <sup>2</sup>, Chao Zuo <sup>1</sup>, Hongjun Wu <sup>1,\*</sup> and Yongtao Liu <sup>1,\*</sup> 

<sup>1</sup> Smart Computational Imaging Laboratory (SCILab), School of Electronic and Optical Engineering, Nanjing University of Science and Technology, Nanjing 210094, China; shijiawu@njust.edu.cn (S.W.); zhaoyalan@njust.edu.cn (Y.Z.); zuochao@njust.edu.cn (C.Z.)

<sup>2</sup> Infection Management Department of Shenzhen Sami Medical Center (Shenzhen Fourth People's Hospital), Shenzhen 518118, China; zhangzitong@ssmc-sz.com

\* Correspondence: wuhongjun2022@njust.edu.cn (H.W.); yongtao.liu@njust.edu.cn (Y.L.)

† These authors contributed equally to this work.

**Abstract:** Exosomes distributed by extracellular vesicles carry various information highly consistent with cells, becoming a new type of biomarker for tumor screening. However, although conventional characterization technologies can quantify size and morphology for exosomes, they are limited in related fields such as function tracing, protein quantification at unit point, and microstructural information. In this paper, firstly, different exosome characterization methods are systematically reviewed, such as dynamic light scattering, nanoparticle tracking analysis, flow cytometry, electron microscope, and emerging super-resolution imaging technologies. Then, advances in applications are described one by one. Last but not least, we compare the features of different technologies for exosomes and propose that super-resolution imaging technology can not only take into account the advantages of conventional characterization techniques but also provide accurate, real-time, and super-resolution quantitative analysis for exosomes. It provides a fine guide for exosome-related biomedical research, as well as application in liquid biopsy and analysis techniques.

**Keywords:** exosome; tumor diagnosis; optical analysis technology; super-resolution microscope



**Citation:** Wu, S.; Zhao, Y.; Zhang, Z.; Zuo, C.; Wu, H.; Liu, Y. The Advances and Applications of Characterization Technique for Exosomes: From Dynamic Light Scattering to Super-Resolution Imaging Technology. *Photonics* **2024**, *11*, 101. <https://doi.org/10.3390/photonics11020101>

Received: 30 November 2023

Revised: 28 December 2023

Accepted: 9 January 2024

Published: 23 January 2024



**Copyright:** © 2024 by the authors. Licensee MDPI, Basel, Switzerland. This article is an open access article distributed under the terms and conditions of the Creative Commons Attribution (CC BY) license (<https://creativecommons.org/licenses/by/4.0/>).

## 1. Introduction

Exosomes, a novel tumor biomarker after circulating tumor cells and circulating tumor DNA [1–3], can be used in tumor diagnosis [4]. Biosignaling molecules of exosomes are exchanged by endocytosis, and thereby tumor cell activities such as growth, metastasis, drug resistance, and immune evasion are regulated [5,6]. Therefore, exosomes have important value in the early diagnosis of tumors, the monitoring of treatment progress, and prognosis as shown in Figure 1 [4,7–9].

Exosomes are membranous extracellular vesicles (EV) secreted by cells with a particle size of 30 to 150 nm [10]. The study found that the function of exosomes depends on the cell type from which they are derived, while it maintains the same genetic material as the donor cells [11]. Different analyses become one of the tumor-specific research targets during exosome activity. For example, exosomes derived from tumor cells carry many types of proteins, such as surface proteins, inclusions, enzymes, etc. Among them, the surface proteins such as CD9, CD63, and CD81 and the inclusion factors such as HSP70 and Alix are representative proteins for the isolation and identification of exosomes [12–14]. The differences in proteins can reflect information exchange between tumor cells and basal cells and between tumor cells and tumor cells, which regulates immune response, migration, differentiation, and other basic cellular functions [15–18]. For example, studies have found that exosomes derived from different cells are different in size, morphology, and composition [19]. The exosomes derived from tumor cells are large and contain more lipids and

outer membrane proteins, which promote tumor cell growth, invasion, and metastasis [20]. The surface proteins of cancer exosomes are often different in different stages, which indicates that these proteins are closely related to the process of cancer. Similarly, the surface proteins of cancer exosomes from different sources are also different, which can be used for the early diagnosis of cancer [21,22]. Research has proven that ADAM10, metalloprotease, CD9, Annexin-1, and HSP70 are enriched in exosomes isolated from the pleural effusion or serum of breast cancer patients [23]. However, the exosomes derived from immune cells are smaller and include a variety of immune molecules, such as cytokines, antigens, antibodies, etc., which could regulate immune responses and antitumor effects [24]. More importantly, quantitative analysis is necessary to identify exosomes accurately. In addition, some studies believe that the morphology, quantity, and concentration of exosomes are different in the process of secretion [25], so real-time tracking and quantification can objectively analyze the delicate mechanism to achieve optimal anti-tumor effect. In conclusion, the morphological characterization and function of exosomes are the basis for exploring the fine physiological information and biochemical mechanisms in cellular biology [26,27].

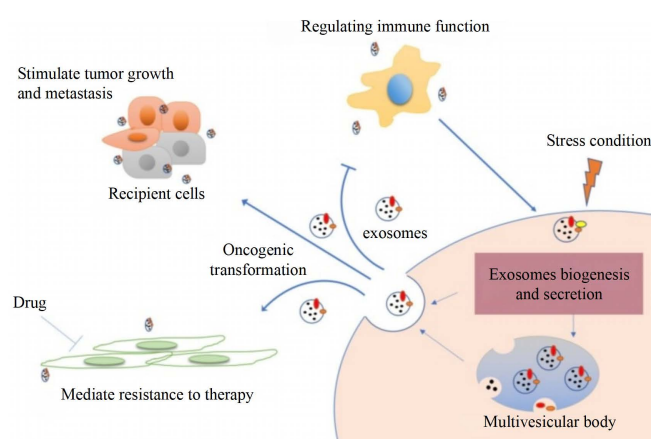


**Figure 1.** Exosome information transfer process and application [4].

Exosomes are emerging biomarkers of tumor liquid biopsy, and therefore it is particularly important to explore their biological information such as function tracing, protein quantification at unit point, and microstructural changes [28,29]. At present, much attention has been paid to their basic characteristics such as concentration, diameter, morphology, and particle tracking in high-throughput samples [30–32]. In this review, we propose that the characterization techniques for obtaining this information are exosome detection techniques. Conventional characterization methods can achieve the basic characterization of exosomes, yet they are subject to certain limitations. DLS can only obtain the size distribution of exosomes but cannot detect concentration [33]. Although flow cytometry (FCM) realizes multi-parameter detection, the analysis results are based on high-throughput samples and cannot obtain the morphological characteristics of a single EV [34]. EM can visually observe the morphological characteristics of a single EV, but it is not suitable for living cells, and the direction is limited in biological research [35]. Therefore, there is an urgent need for an exosome detection technique that can preserve the fluorescence specificity and achieve high-throughput sample single-molecule detection. In recent years, researchers have paid more attention to fluorescence microscopy. The fluorescence microscope has the advantage of live cell imaging and specific labeling; however, its resolution ranges from 200 nm to 500 nm, which cannot be applied to detecting exosomes. Therefore, how to improve the imaging resolution of optical microscopy and apply it to the imaging observation of subcellular structures such as exosomes has become a research hotspot in recent years. With the development of fluorescence microscopy, super-resolution imaging technology breaks through the diffraction limitation, which is conducive to the field of exosomes [26,36]. Compared with others, it has the advantages of high resolution, specific detection, and

live-cell imaging to realize the qualitative and quantitative analysis of proteins of living or fixed cells and track the mechanism of exosomes [36].

In order to better guide the research on exosomes, we systematically discussed and compared characterization techniques for exosomes. This review system elaborates on the principles and applications of conventional characterization technologies for exosomes such as dynamic light scattering (DLS), nanoparticle tracking analysis (NTA), flow cytometry (FCM), electron microscopy (EM), and scanning electron microscopy (SEM), as well as super-resolution technologies represented by stochastic optical reconstruction microscopy (STORM), photoactivated localization microscopy (PALM), stimulated emission depletion (STED), and structured illumination microscopy (SIM). More importantly, this paper discusses the medical problems and characterization techniques of exosomes from morphological characterization to the functional expression of exosomes, from complex samples to single exosomes, and from multiple protein quantification to a single protein of a single exosome. The mechanism and information communication of exosomes were systematically settled from the perspective of technology development, which provides more systematic and comprehensive guidance in the field of basic research.

## 2. Conventional Characterization Technologies

Due to the unique biological function of exosomes, an increasing amount of basic research is being concentrated on it [37–41]. Characterization technologies play important roles in the study of exosomes [30]. Generally speaking, various approaches for analysis are categorized into two primary types: biochemical analysis and physical analysis. Biochemical analysis mainly determines the source and composition of exosomes, including Western blot and enzyme-linked immunosorbent assay (ELISA), in which the specific binding of antibody antigens decides the effect qualitatively or quantitatively [42]. However, the disadvantage is that the morphological characteristics and concentration of exosomes cannot be obtained. We introduce electron technologies such as tunable resistive pulse sensing (TRPS) and electron microscope (EM) in the first section. Then, we compare optical analysis technologies including dynamic light scattering (DLS), nanoparticle tracking analysis (NTA), and flow cytometry (FCM). Last but not least, we discuss the main parameters of different technologies, providing technical guidance for the fundamental research on exosome characterization.

### 2.1. Tunable Resistive Pulse Sensing

Tunable Resistive Pulse Sensing (TRPS) is based on Coulter's principle. The suspension was mixed in the electrolyte, which could go through the nanopore chip with a specific aperture. The resistance between the two electrodes inside and outside changes instantaneously at the moment of passing through the nanopore, the result of which is a pulse signal as shown in Figure 2a. The intensity and frequency of the signal are related to the size and number of exosomes. The expression of exosomes was counted by the pulse signal. In 2014, Maas proposed a method to characterize the concentration and size of EVs by the TRPS based on the qNano system [43]. In 2017, researchers pointed out that TRPS has promise in the quantitative and dimensional analysis of single-particle EV [44]. In 2018, Durak-Kozica analyzed EVs from endothelial cells for a short time and found that the diameter of EVs was  $121.84 \pm 0.08$  and  $115.82 \pm 0.96$  nm from microvascular and big vessels, respectively [45]. This technology enables the efficient quantification of size and number, which cannot be specifically analyzed for exosomes due to the principle of potential pulses.

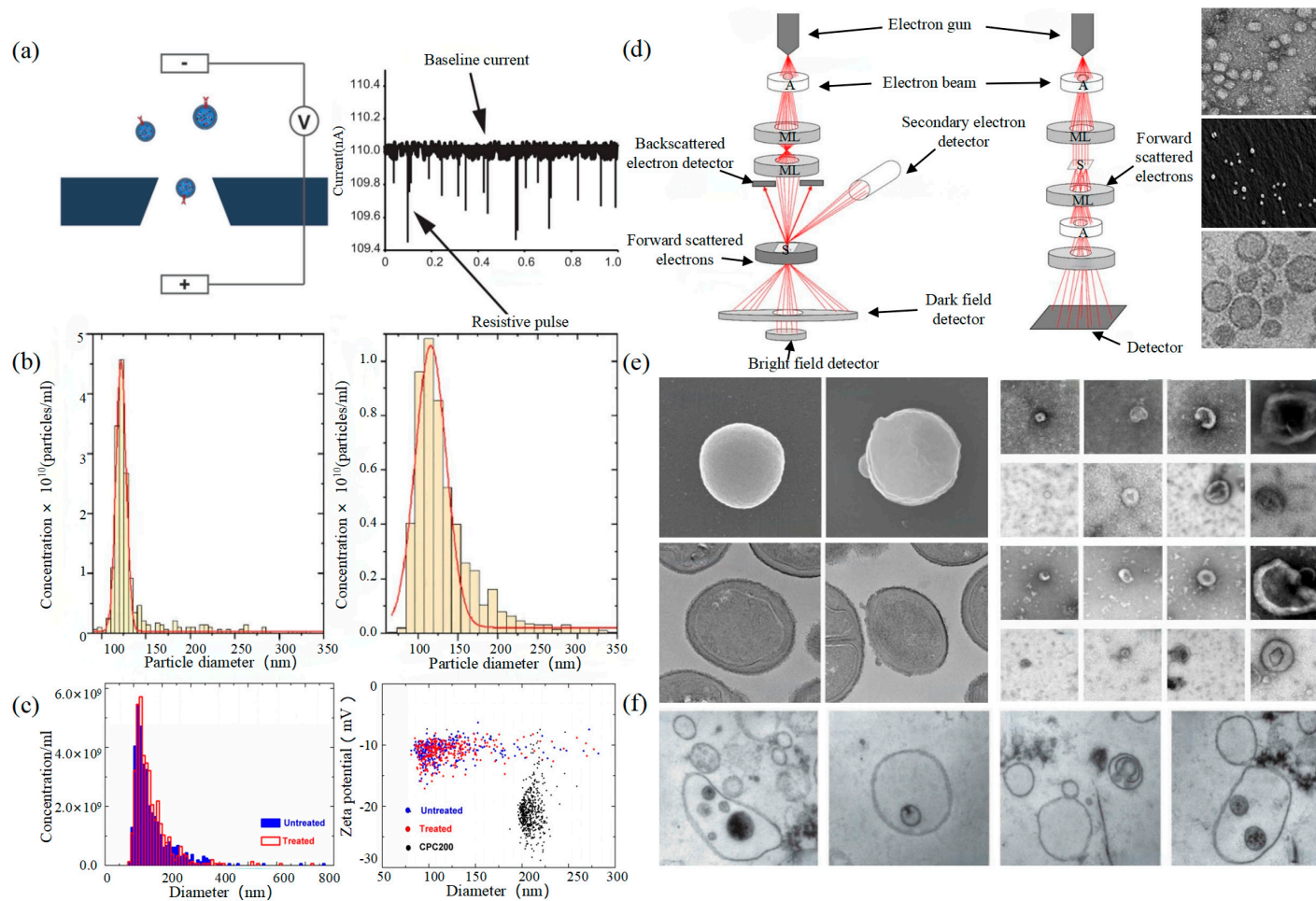


**Figure 2.** TRPS and EM (a) The principle of TRPS [43]. (b) TRPS reveals the size distribution of EVs derived from the TIME cell line (left) and the HUVEC line (right) [45]. (c) Particle concentration and size measurements for EV samples before and after INTERCEPT treatment (left), Simultaneous size and zeta potential measurements of untreated and INTERCEPT-treated EV samples and carboxylated polystyrene standard particles (right) [46]. (d) The principle of SEM (left) and TEM (middle) [47] and EVs scans of TEM [48], SEM [49], cryo-TEM [50] (right). (e) EM images of *S. aureus* without EVs and with EVs (left) [51]. Examples of EM images of individual cup-shaped EVs of different origins [19]. (f) Multivesicular bodies (MVBs) contained in cultured HMC-1 cells and extracellular vesicles in the surrounding growth medium [52].

## 2.2. Electron Microscope

Electron Microscope (EM) is the most direct method to measure the size and morphology of a single EV [42]. It is divided into scanning electron microscope (SEM), transmission electron microscope (TEM), and cryo-transmission electron microscope (cryo-TEM). It is noted that EM can characterize the particle morphology and size of a single EV [53,54].

The outer membrane of EVs was imaged by a focusing electron beam, the results of which were secondary electrons with different emission amounts. The principle is shown on the left of Figure 2d. Min Kyo Jung et al. observed the detailed structure and specific protein of EVs stained by the negative staining technique [55]. Boz et al. observed the mechanism and morphology of hbEV by SEM [56]. Sokolova et al. obtained the morphological characteristics of exosomes derived from different cells including HEK110T, ECFC, and MSC [57]. The principle of TEM is that the electron beam collides with atoms of EVs, and the scattering angle is converted to acquire the changes in structure, as shown in the middle of Figure 2d. Compared with SEM, TEM has a higher resolution and can realize the imaging analysis of a single EV at the nanoscale [58]. Liu et al. successfully characterized exosomes extracted from breast tumor cells including their morphology and distribution [59]. Park et al. found the morphology of EVs derived from prostate cancer cells (PCa) was round and that the number of these EVs was significantly higher than that of normal cells [60]. It is worth noting that sample protocol is complicated and that the sample is in a vacuum during the process of imaging. In order to reduce the complexity of the protocol, the researchers further developed cryo-TEM to maintain the integrity and authenticity of the sample to the greatest extent [52]. This element changes the structure of the exosome from a round to a cup-like shape as shown in the right of Figure 2d. Conde-Vancells et al. realized the morphological characterization of exosomes derived from hepatocytes [50]. Kurtjak et al. identified the single, double, and multi-membrane morphology of CSF extracellular vesicles by combining cryo-TEM with atomic force microscopy (AFM) [61]. This proves that the cryo-TEM technique can not only restore the EV shape but also allow the analysis of the EV interior.

## 2.3. Dynamic Light Scattering

Dynamic light scattering (DLS) is an optical analysis method for measuring the size and distribution of sub-micron particles, and its basic principle is shown in Figure 3a. The Brownian motion of the particles causes the change in the light scattering signal, which is monitored by a digital autocorrelator to calculate the diffusion velocity and particle distribution of the particles [62]. The motion rate of small particles is higher, and its intensity fluctuation is larger. As a result, there is a swift and pronounced decline in the correlation curve. The sensitivity and FOV of DLS are better than the above papers, which can realize the basic characterization of large-size exosome nanoparticles. For smaller particles, the behavior of self-polymerization interferes with the light-intensity signal. Thus, it is impossible to realize the precision analysis and detection of high-concentration samples. In 2009, Lawrie et al. used DLS to characterize the size distribution of EV derived from red blood cells [63]. DLS analyzes all particles in a sample simultaneously, and therefore the information on the number or concentration of a certain category of particle cannot be provided [64]. For example, DLS provides a clear range of the diameter of EVs derived from ovarian cancer cells, but the concentration is difficult to analyze [65]. Therefore, DLS technology is often combined with other technologies to complete the characterization of EVs. For example, Tajik T combined DLS technology with electron microscopy, showed cannabis-derived EVs (CDEVs) can be considered exosome-like nanovesicles, and highlighted that CDEVs can be an ideal natural vehicle for bioactive phytocannabinoids, promoting the research of EVs in cancer diagnosis [66].

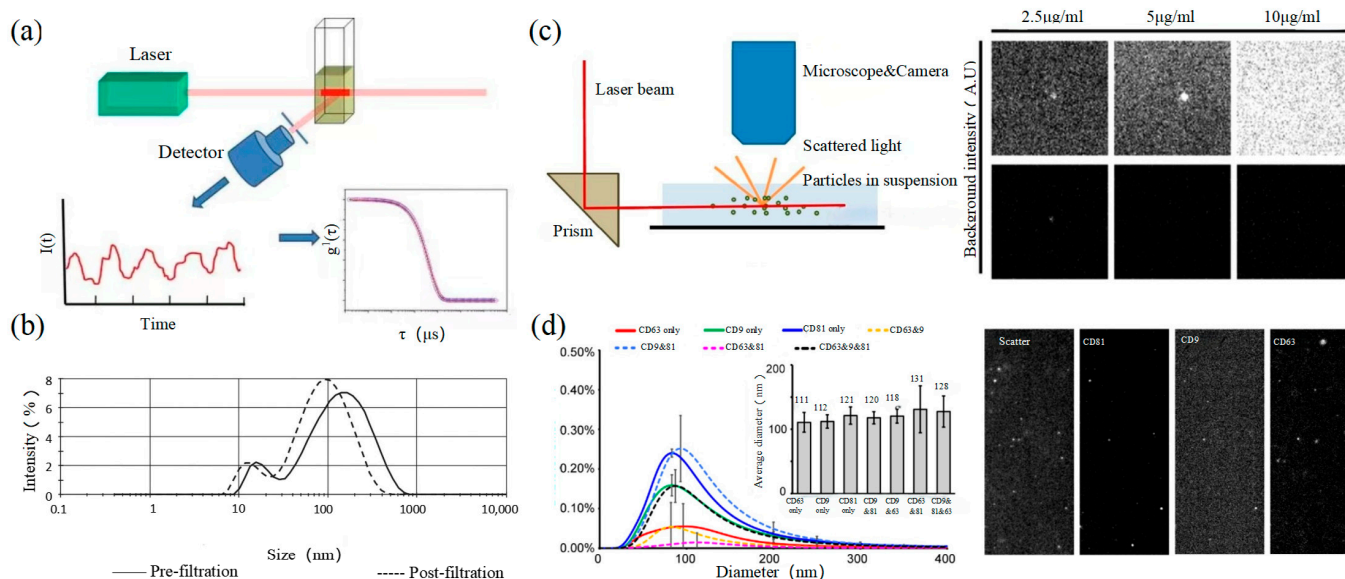


**Figure 3.** DLS and NTA (a) The principle of DLS [67]. (b) DLS to characterize the size distributions of microparticles within fresh-frozen plasma [68]. (c) The principle of NTA (left) [69] and EVs of fluorescent labeling on extracellular vesicles and fluorescence detection ability of NTA [70]. (d) Size distributions of three CD markers (CD9, CD63, and CD81) in multifluorescence by NTA (left) and fluorescent images of particles by NTA (right) [70].

#### 2.4. Nanoparticle Tracking Analysis

Nanoparticle tracking analysis (NTA) is an optical method to assess nanoparticles [71]. When the laser irradiates a single nanoparticle, light intensity scattered from the sample is captured by a high-speed camera as shown in the left of Figure 3c. Compared with DLS, NTA can locate and track a single nanoparticle, so this technology has advantages in analyzing the particle size of complex samples. It is worth mentioning that NTA has the ability of fluorescence analysis. Different fluorescent particles can be measured by the relevant parameters, which can identify the sizes of various exosomes at the same time. In 2011, Dragovic et al. applied quantum dot-labeled fluorescent cell tracking peptide with NTA to confirm the origin of common vesicles in plasma [72]. In 2014, Gardiner et al. novelly proposed the refractive index (RI) counted by the relative light scattering intensity (rLSI) could identify the heterogeneity of EV [73]. Saari, H. et al. achieved the distribution of EV in different subpopulations of prostate cancer cells [74]. Huilin Shao et al. tracked the dynamic activity of EVs' distribution with NTA [75].

#### 2.5. Flow Cytometry

Size and morphology are the basic parameters for the characterization of exosomes. The characterization of functional parameters such as surface protein quantitative expression and signal transduction mode is of paramount importance. Flow Cytometry (FCM) realizes the rapid multi-parameter quantitative analysis of cells or submicron particles based on light scattering changes, and its basic principle is shown in Figure 4a. Scatters of light from particles suspended in a sheath stream reflect the size and density of the cells or particles, and they were acquired by a detector array. At the same time, the specific gene expression, protein expression, enzyme activity, ion concentration, and other biomolecular substances labeled by fluorescent dyes were specifically measured by different channels.

The sensitivity of traditional flow cytometry is limited to 300 to 500 nm [76], so it is obviously difficult to measure exosomes. Yan Xiaomei's team developed nFCM by combining Rayleigh scattering with sheath flow single-molecule fluorescence detection technology, which enables the high-throughput analysis of exosomes with a size of 40 nm, as shown in Figure 4b [77,78]. Compared with traditional flow cytometry, the scattered light

detection sensitivity of nFCM is improved by four to six orders. More importantly, nFCM can detect the scattered light signal of a single nanoparticle at a rate of 10,000 particles per minute [79]. The advantages of this technology are high sensitivity and high throughput, which is suitable for analyzing the size, concentration, and biochemical properties of EVs. In 2022, Haisheng Liu et al. provided evidence for the relationship between DNA and EVs, which confirmed that genetic information in EVs is consistent with cells [78].

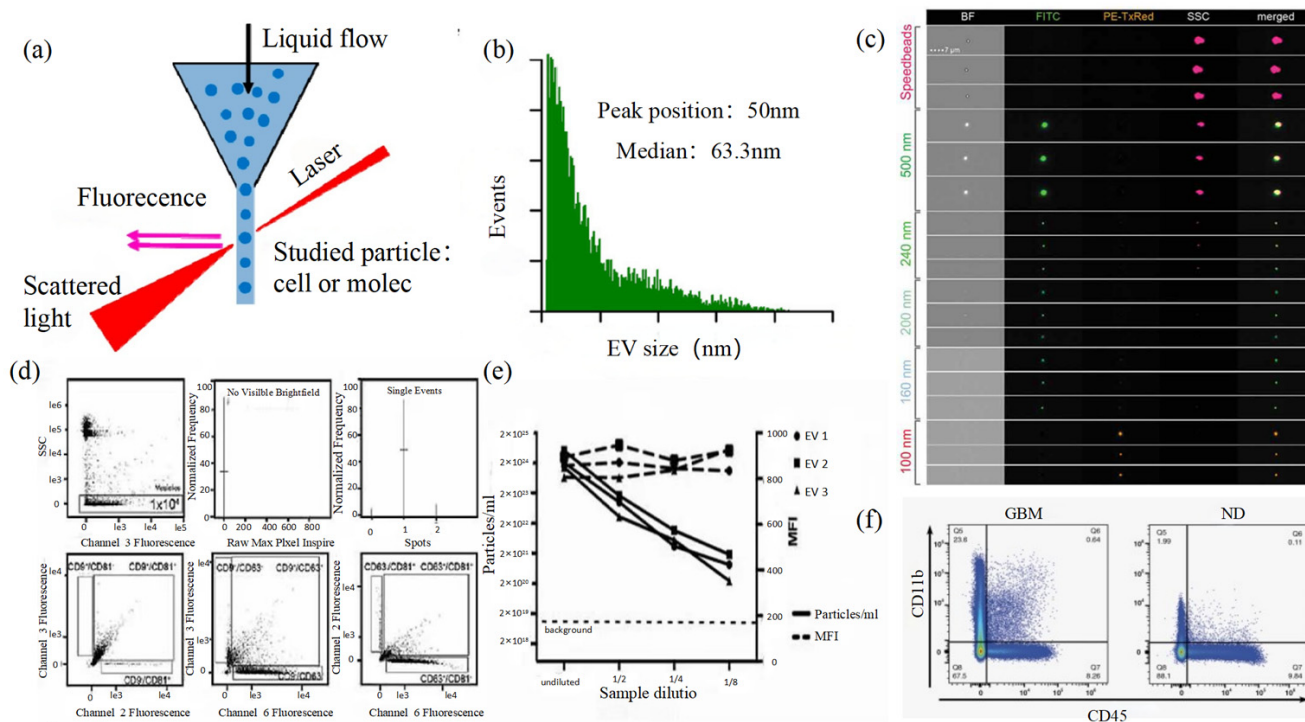


**Figure 4.** FCM (a) The principle of FCM [69]. (b) Histogram of particle size for an EV sample of HCT-15 cells [78]. (c) Heterogeneous fluorescent beads were analyzed by FCM [80]. (d) FCM detects CD9, CD63, and CD81 positive EVs [80]. (e) FCM analyzes the EV concentration and mean fluorescence intensity (MFI) of the anti-CD9-PE-stained EVs of the three individual EV preparations [80]. (f) Analysis of plasma EVs expressing CD45 and CD11b in GBM and normal donors [81].

The detection method based on electronic technology and optical technology can realize the analysis and quantification of exosomes and provide the necessary quantification technology for the basic research of exosomes. The comparison of the advantages and disadvantages of each method is shown in Table 1. FCM and TRPS can achieve high-precision detection for high-throughput samples. EM is the only characterization method that can reveal the three-dimensional structure of exosomes, but it is not suitable for the detection of high-throughput samples because of the sampling protocol. NTA and FCM enable the functional evaluation of exosomes by fluorescence-specific labeling. According to Table 1, it is obvious that FCM can achieve the structural and functional characterization of exosomes. However, the analysis results are based on high-throughput samples, and the morphological characteristics of a single exosome cannot be obtained easily, so it is difficult to apply in more biomedical fields. Although EM could achieve imaging for samples at low concentrations, cumbersome protocols place greater demands on researchers.

**Table 1.** Comparison of conventional characterization techniques.

	Detection Range	Direct Analysis	Accuracy	Single Molecule Tracking	Sample Flux	Specificity	Multi-Parameter Characterization	References
TRPS	>30 nm	No	High	No	High	No	No	[43–46]
EM	>5 nm	Yes	High	Yes	Low	No	No	[35,53,54]
DLS	5–2000 nm	No	Low	No	High	No	No	[62,63,67]
NTA	50–1000 nm	No	Normal	Yes	High	Yes	No	[69,71]
FCM	300–500 nm (nFCM is about 50 nm)	No	Normal	Yes	High	Yes	Yes	[42,76,77]

### 3. Super-Resolution Imaging Technology

The development of modern biology has promoted the rapid progress of microscopic imaging technology. Due to the limitation of optical diffraction, the minimum resolution of the traditional optical microscope is about half of the wavelength of incident light. Therefore, scientists have been constantly trying to break through it. The resolution of super-resolution imaging technology is below 200 nm, which obtains the same level of resolution as EM. Super-resolution microscopy can achieve real-time super-resolution imaging for organelle structure, interaction, protein function, etc. It provides a new analytical method for cell biology and breaks through the biomedical research status from the nano-scale.

At present, super-resolution imaging technology is divided into two categories. One is a single molecule localization imaging technique (SMLM) based on the random switching of the excited light of the fluorophores between on and off states, which includes stochastic optical reconstruction microscopy (STORM) and photoactivated localization microscopy (PALM). The other is the super-resolution imaging technology achieved based on light field regulation such as stimulated emission depletion (STED) and structured illumination microscopy (SIM). In this section, the application and development of super-resolution technology in exosomes are discussed.

#### 3.1. Single Molecule Localization Imaging Technology

The basic principle of SMLM is based on the flicker of a single fluorescent molecule to locate a single molecule and then reconstruct super-resolution images. Compared with other technologies, SMLM has the advantages of low phototoxicity and low cell damage. It is more suitable for living cells, thus becoming a new super-resolution analysis method for exosomes in vivo observation. SMLM opens a new observation perspective for exosome-related studies.

##### 3.1.1. Stochastic Optical Reconstruction Microscopy and Photoactivated Localization Microscopy Technology

PALM and STORM technologies are classical technologies in SMLM. In 2006, Eric Betzig et al. proposed the PALM technology [82], and Xiaowei Zhuang et al. proposed the STORM technology [83] at the same time. Both of them are based on single-molecule localization technology to achieve the super-resolution imaging of subcellular structure molecules. One of the key elements is the switched fluorophores. For example, PALM uses photoactivated green fluorescent protein (PA-GFP) to label the protein and irradiate the cell surface with different lasers so as to cause the fluorescence molecule cycle to complete the excitation localization process, as shown in the left of Figure 5d. STORM relies on Cy3-Cy5 to change the status of Cy5 to achieve optical switching. Therefore, the intensity should be controlled at a low level as shown in Figure 5a. With the application of fluorescent probe screening, van de Linde et al. found that Alexa Fluor647 does not rely on other dyes to activate light, but it could directly achieve the switching process of fluorophores by high-intensity excitation lights [84]. That means direct stochastic optical reconstruction imaging (dSTORM) can be achieved.



One of the key points is the spatial and temporal resolution for SMLM. That requires more than 10,000 frames of images during the process of reconstruction, which needs much more time. The rapid development of EMCCD cameras has greatly improved imaging speed. In 2011, Zhuang Xiaowei’s group pictured extracellular vesicles with a high-speed EMCCD. The temporal resolution was improved to 0.5 s, which means that STORM has the potential to monitor live cell imaging in real-time [85]. Zhuang et al. also proposed a high-density algorithm based on compressed sensing (CSSTORM), which successfully reduced the original data needed in constructing a super-resolution image to 169 frames [86]. In 2020, Qu’s team combined noise-corrected principal component analysis (NC-PCA) with CSSTORM to decrease the original data noise, the results of which were that the hyperfine structure and dynamic processes of mitochondria were successfully observed in living Hela cells at different time points [87]. In addition, SMLM combined with deep learning also greatly improves temporal resolution. In 2021, Wei Ouyang et al. combined PALM with deep learning, reducing the number of sampling frames from 30,000 to 300 frames and increasing the time resolution of the system by 100 times [88]. All of this means that the development and application of algorithms play an important role in improving the temporal resolution of SMLM technology.

The optimization of the single-molecule localization algorithm is a great help to the development of SMLM technology. Meanwhile, the development of fluorescent probes also promotes the development of SMLM. With the combination of the above, spatial resolution is greatly improved, even reaching less than 10 nm [89], which makes it possible for us to observe the fine structure of exosomes through optical microscopy.

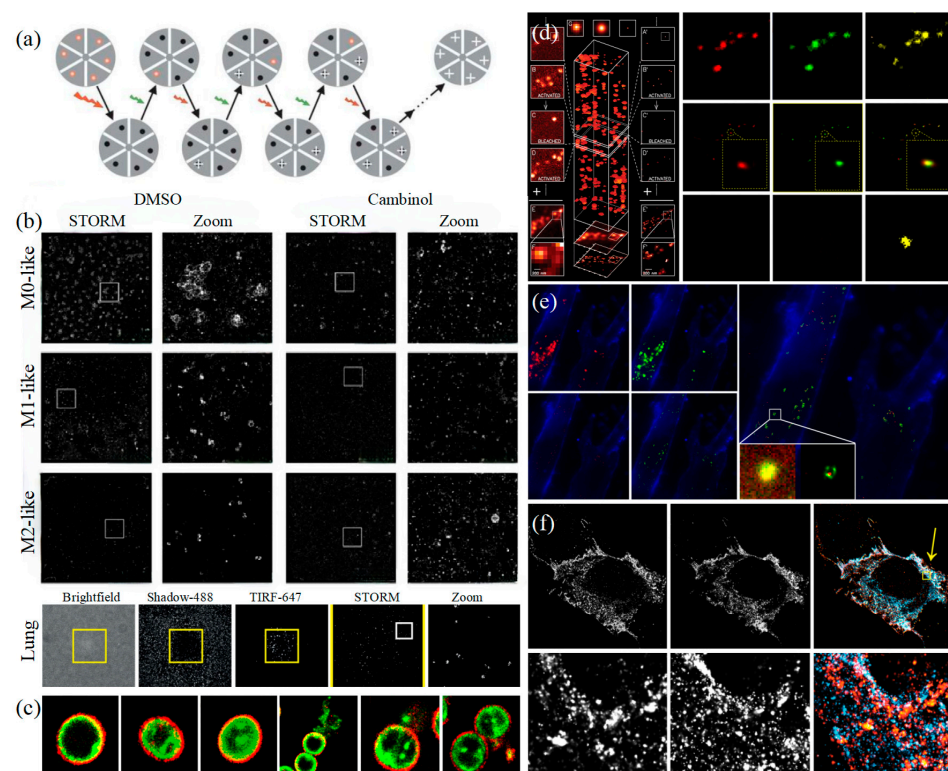


**Figure 5.** STORM and PALM (a) The principle of STORM [83]. (b) STORM observes that EVs colocalize with wells in the actin reticulum and can be inhibited by Cambinol (above), and human lung macrophages secrete EVs upon activation through their FcγRI (below) [90]. (c) Multi-color STORM images for the various compositions of EVs in gram-positive bacteria [51]. (d) The principle of PALM [82] (left) and Dual-color super-resolution imaging of CD63 and HER2 in SKBR3-derived exosomes [91] (right). (e) PALM/STORM was used to observe the colocalization of SKBR3 exosomes and MRC-5 lysosomes [91]. (f) CD63-GFP and CD81-mCherry U-2 OS expressing cells were visualized by dSTORM [48].

In 2011, Zhuang's team used the stage-specific neurite-associated protein (SNAP) label to label the Alexa Fluor 467 optical switching probe to clathrin in living BS-C-1 cells. STORM technology was successfully used to obtain a 30 nm horizontal resolution and a 50 nm vertical resolution [85]. In 2012, Shim et al. determined the STORM membrane probe for live cell imaging through a large number of experiments and performed the super-resolution imaging of organelle membranes in live cells, reaching a spatial resolution of 20~60 nm [92]. In 2018, Zong Shenfei et al. discovered that silicon quantum dots (Si QD) have fluorescent scintillation behavior and applied them as SMLM imaging nanoprobe to stain CD63 of breast cancer cell (SKBR3)-derived EVs using CD63 aptamers fused with Si QD, achieving an imaging accuracy of about 30 nm. They demonstrated that Si QD can be used for the SMLM imaging of small objects such as exosomes. Moreover, Si QD has the characteristics of high biocompatibility and low cytotoxicity, which makes it a better choice of fluorophores for SMLM live cell imaging [93].

At present, SMLM provides a fast and high-precision optical detection method for exosome structural characterization. The implementation of high-speed STORM/PALM makes it possible to analyze the functional communication effects of intracellular or intercellular information and substance exchange in exosomes. In 2016, Chen et al. verified the possibility of PALM/STORM in exosome imaging by labeling extracellular proteins [91]. On the one hand, the imaging of exosomes obtained by PALM/STORM can be obtained with authenticity. On the other hand, bicolor STORM imaging revealed the intercellular transport of exosomes, suggesting that cellular exosome uptake depends on endocytosis and phagocytosis. In 2018, Chen et al. observed the entire process of the transport of entotic exosomes to lysosome degradation, with a time resolution of 4 s. It has been verified that this time resolution is sufficient to reveal the movement process of exosomes [94]. At the same time, they also observed that the contents of exosomes reached the cytoplasm through the endocytosis process and revealed the mechanism of the action and movement of exosomes in a more detailed manner. Those results effectively promoted the development of biomedical research on exosomes as drug carriers. In 2019, Mondal et al. achieved the effective tracking of EV by PKH67 dye to label Neuroplasma-derived EV's surface markers such as CD63 and inter-vesicle markers such as TSG101 and HSP70 and observed that EV was effectively internalized by recipient cells [95]. In 2022, Jeong et al. successfully visualized the EVs biogenesis of Gram-positive bacteria through super-resolution imaging technology, which examined the ultrastructure and three main mechanisms of biogenesis that emphasized the important role of cell wall degradation in these mechanisms [51]. In the same year, McNamara et al. visualized hundreds of single EVs in 3D and digitally located the four transmembrane proteins (CD9, CD63, and CD81) on the surface of EVs, which revealed the heterogeneity of EVs [48]. In 2023, Saftics et al. comprehensively evaluated EV subsets in human plasma and compared EV in the plasma of pancreatic cancer patients with healthy plasma and found that there were unique EV subsets in pancreatic cancer patients, which was beneficial to the research of EV as a basis for cancer diagnosis [96].

SMLM technology also provides direct evidence for EVs as a novel tumor biomarker. First, it confirmed that EVs are related to the pathological process of tumor metastasis. Oleksiuk et al. demonstrated for the first time the visualization of miRNA in the exosomes of colon cancer cells (SW480) at the single-molecule level in 2015. Most of the highly metastatic SW480 exosomes have higher molecular weight miR-31, which has a profound impact on the identification of key metastatic subgroups in heterogeneous cancer cell populations [97]. In 2018, Zong Shenfei's team tracked the miRNA of exosomes in HeLa cells, which is crucial for studying the influence of exosomes on cancer cell metastasis [94]. Recently, the team also proposed that exosomes were amplified by combining amplification microscopy (ExM) with SMLM to achieve a localization accuracy of about 30 nm. Successfully, they observed the nanoscale substructure of proteins on the exosomes of human breast cancer (SKBR3) cells and HeLa cells, providing a new idea for visualization exosome super-resolution imaging research [98]. What is more, the research of EVs by SMLM technology shows great potential in cancer diagnosis. In 2019, Lennon et al. evaluated EVs in cells and

plasma by dSTORM, effectively distinguishing pancreatic cancer-enriched EVs in cancer diagnosis [99]. In 2022, Dechantsreiter et al. located a single EV derived from human macrophages (MDM) by combining STORM with proteomic analysis, revealing the EV content of different sizes and the differences between EVs secreted by different MDM. The study found that the frequency and intensity of HLA-DR expression in the MMD-secreted EV derived from the lungs of cancer patients was higher, suggesting the enrichment of macrophages in the lungs of cancer patients [90]. In the same year, Wei et al. proposed a fluorescence detection method for EDIL3-overexpressed exosomes through SMLM and proposed that EDIL3-overexpressed exosomes are novel biomarkers for the early diagnosis of triple-negative breast cancer (TNBC), which have great potential in the clinical diagnosis of TNBC [100].

### 3.1.2. DNA-PAINT Technology

Similar to the STORM/PALM technology, DNA-PAINT also achieves super-resolution imaging by controlling the flicker of individual fluorophores. In 2014, Ralf Jungmann et al. proposed the DNA-PAINT technology, which uses reversible binding between complementary DNA sequences to produce an effect similar to the “flicker” of fluorescent molecules [101]. In double-strand DNA, one strand is connected to the fluorophores, called the imager strand, and the other is connected to the target molecule, called the docking strand. Due to the highly specific binding of the double-strand DNA, the imaging strand and the docking strand are bound spontaneously, producing single-molecule fluorescence in the focal plane [102] as shown in Figure 6a. In addition, multi-channel fluorescence imaging can be realized by different proteins labeled with various docking strands.

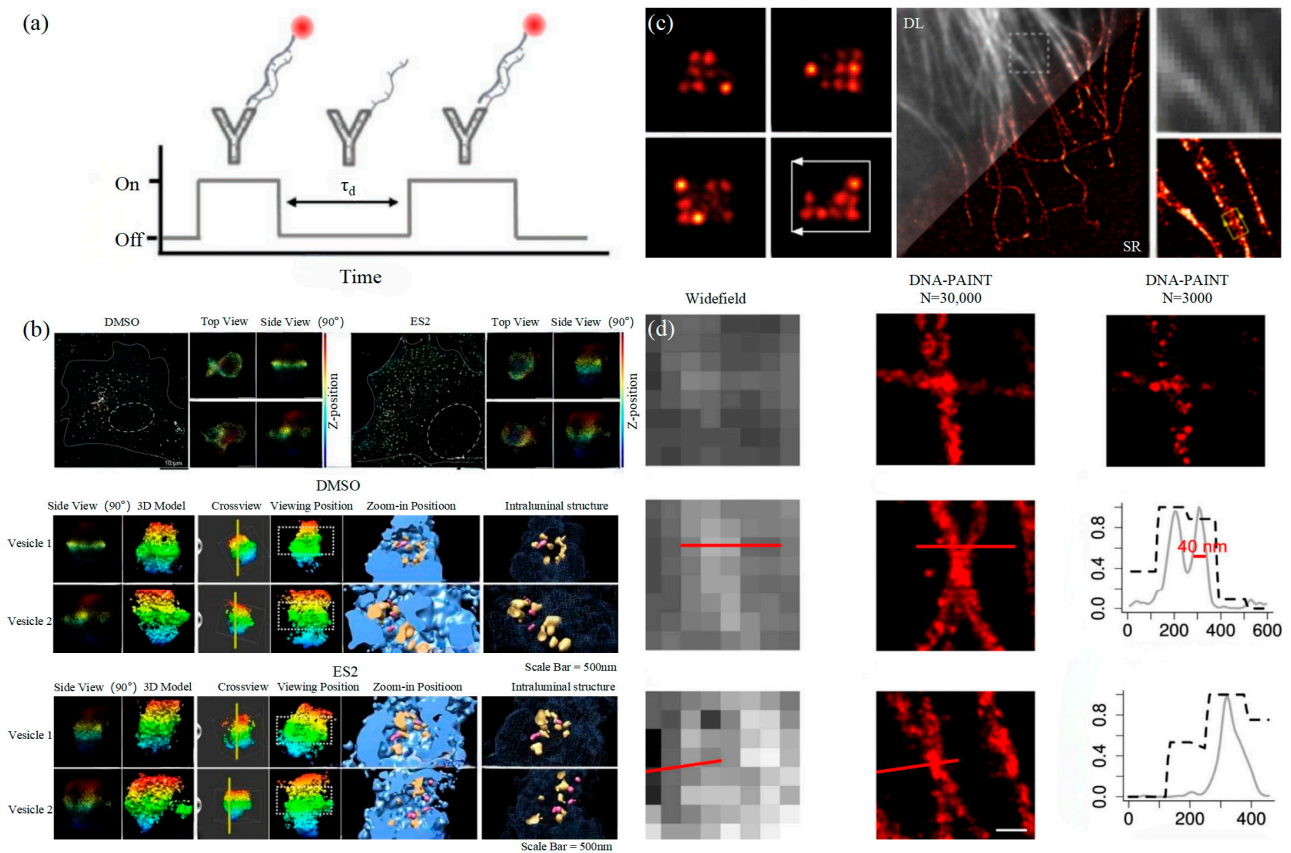


**Figure 6.** DNA-PAINT (a) The principle of DNA-PAINT [103]. (b) 3D DNA-PAINT images of COS-7 cells treated with DMSO or ES2 [104]. (c) Representative super-resolution images of 20 nm grid structures (left) and Diffraction-limited (DL) alongside the super-resolution (SR) of the microtubule network in a HeLa cell [105]. (d) Comparison of the widefield images and DNA-PAINT images [106].

The DNA-PAINT technology focused on reducing the resolution to the molecular level early. Then, it focused on the limitation of long acquisition times [107]. Long collection time is a basic limitation of SMLM technology, which is due to the need to collect enough photons to determine the central position of the fluorophores [108]. The common idea is to increase the binding frequency at a high concentration of the docking strand, but the concentration of the imaging strand influences the SNR of technology [109]. In 2017, Auer et al. developed a FRET-based imaging probe, which not only alleviated the limitation of the concentration of the imaging strand and successfully increased the image acquisition speed by several orders of magnitude but also performed a 30 s super-resolution imaging of microtubules, demonstrating usability in living cell imaging [105]. In 2020, Strauss et al. proposed a method to optimize the docking strand sequence, which increased the image acquisition speed of DNA-PAINT by 100 times compared to traditional methods, and then they extended this method to six orthogonal sequence mods to achieve fast multiple imaging [110].

Proteins on exosomes can be quantitatively analyzed with high precision by DNA-PAINT. The different contents of proteins carried by exosomes such as CD9, CD63, CD81, HER2, EpCAM, and EGFR could achieve the classification of the course of tumorigenesis [111]. Chen et al. combined DNA-PAINT with machine learning to identify tumor cell types in two steps [103]. The first step is to distinguish between healthy cells and tumor cells and then to perform cross-typing on different types of tumor cells, among which the comparison results of breast cancer and pancreatic cancer show that the system can accurately and quickly distinguish the two types of cancer, which makes it possible for exosomes to achieve an early diagnosis of cancer through optical detection. Coincidentally, Zhu et al. also combined machine learning with DNA-PAINT to develop a neural network based on U-Net, U-PAINT, which successfully compressed tens of thousands of frames of raw data required for traditional DNA-PAINT imaging to one-tenth of its original size and is expected to achieve faster DNA-PAINT imaging of living cells in the future [106]. In addition, Bai et al., in a study on exosome biogenesis and release in head and neck cancer cells (HNC) in 2021, pointed out that extracellular sacs may be involved in exosome biogenesis [112]. Recently, a 3D super-resolution imaging using DNA-PAINT examined the multivesicular endosomes (MVE) of COS-2 cells and confirmed that phosphoinositol mediated extracellular vesicles to guide MVEs' fusion with the plasma membrane to release exosomes [104].

### 3.2. Stimulated Emission Depletion Technology

In 1994, Hell et al. proposed stimulated emission depletion technology (STED) for the first time in theory. The principle of STED is that two laser beams are used for microscopic imaging, with one as excitation light for photon excitation and the other as loss light, which is a ring laser with zero central intensity [113]. The loss light should be coaxial with the excitation light, and the wavelength should match the emission wavelength of the fluorescence molecule as shown in the left of Figure 7a. STED is a super-resolution imaging technology developed based on laser scanning confocal microscopy. Fast, direct imaging characteristics and a nanoscale observation scale are ideal for living cell research. However, the resolution of STED is affected by the ratio of lost optical power to probe saturation excitation power. The higher the relative power, the higher the imaging resolution, but it will also cause the rapid photobleaching of fluorophores, causing serious photodamage to cells. Therefore, the application of STED to live cell super-resolution requires the development of fluorescent probes.

Many research teams are committed to developing photobleach-resistant fluorescent probes that can be used in STED live cell imaging studies. In 2016, Butkevich et al. discovered Rhodamine dye capable of penetrating cell membranes and used it to achieve the STED super-resolution imaging of live cells [114]. However, the dynamic monitoring of the dynamic processes of living cells is of great significance in biological research. In 2019, several new probes were developed by the Pajk team for STED live cell imaging. Compared

with the same type of fluorescent probes on the market, they not only have higher resolution but also have no obvious toxicity and can enter cells relatively quickly, promoting the super-resolution imaging and dynamic monitoring of living cell organelles [115]. In the same year, Valcz et al. specifically tagged CD63 and ALIX proteins and determined that the in situ release of EVs from colorectal cancer cells was caused by the fusion of MVB with plasma membrane by STED-assisted detection [116]. On this basis, the researchers further sought to improve the resolution of STED. In 2020, Yang et al. developed an enhanced aromatic acid variant dye (MitoESq-635) and successfully achieved the STED imaging of the mitochondrial inner membrane of HeLa cells with a resolution of 35.2 nm thanks to the dye's low saturation and high light stability, promoting STED research on the long-term imaging observation of tumor cells [117]. In addition, Alvelid et al. developed a new adaptive microscopic imaging method called etSTED in 2022, which combines fast wide-field imaging with STED imaging to achieve 3DSTED nanoimaging acquisition, and successfully observed different EVs and membrane fusion events in tumor cells, promoting the exosome study of STED [118]. In the development of fluorescence probes, upconversion nanoparticles (UCNPs), as a new class of nonlinear optical probes, can emit stable and bright visible light at various optional wavelengths under near-infrared excitation and have single particle sensitivity; therefore they can be used in optical microscopy imaging [119]. In 2020, Yongtao Liu successfully used UCNPs to track single nanoparticles inside tumors with a resolution of 55 nm of STED and proposed an application to track single nanoparticles and monitor drug release in the 3D multicellular environment [120]. In 2022, Huang et al. applied UCNPs to the STED super-resolution imaging of EVs by specifically binding UCNP to antigens on tumor EVs, reaching a resolution of 41.9 nm and successfully distinguishing neighboring UCNPs on a single EV. As the size of UCNP decreases, the number of UCNP observed on a single EV increases. Although the absolute characterization of the number of all antibodies cannot be achieved, the trend in their number can be characterized, which can be considered for the detection of tumor growth and cancer metastasis in the future [121]. In 2023, Liu et al. used UCNPs to successfully achieve the highest resolution of STED, i.e., sub-40 nm, with the assistance of nonsaturated confocal super-resolution results [122]. At present, the research on UCNPs is still in progress, which will promote the application of STED to EV imaging.

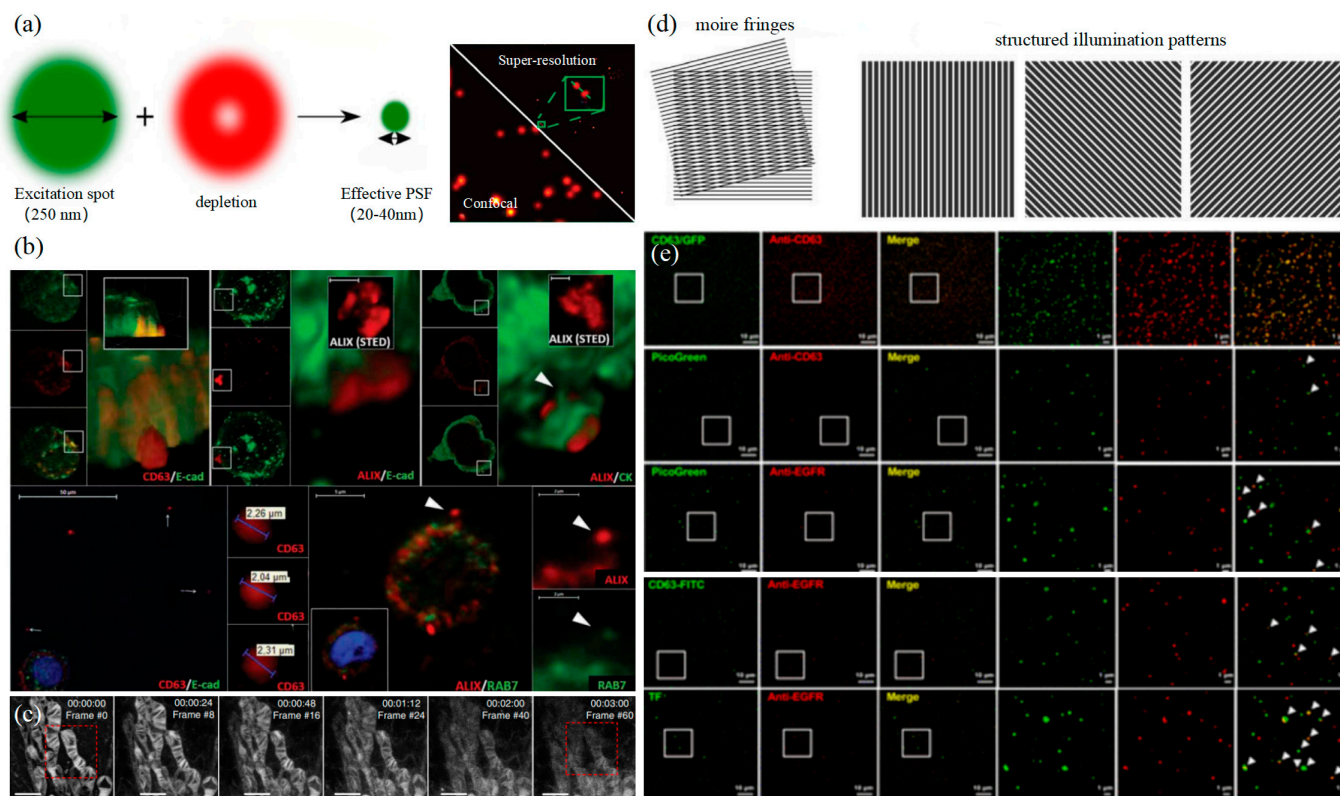


**Figure 7.** STED and SIM (a) The principle of STED (left) [123] and characterization of single EVs by UCNP labeling using STED (right) [121]. (b) Visualization of extracellular sEVCs in HT29 colorectal carcinoma cell [116]. (c) Time-lapse STED imaging of the mitochondria [117]. (d) The principle of SIM (left) [123]. (e) SIM resolution was validated by a complete co-localization between genetic tag-based (CD63-GFP) and immunofluorescent imaging for the CD63 [124].

### 3.3. Structured Illumination Microscopy Technology

Structured illumination microscopy technology (SIM) is a super-resolution imaging technology based on frequency domain modulation proposed by Gustafsson in 2000 [125]. A Moire fringe is used to transfer high-frequency information beyond the system cutoff frequency to the low-frequency part to realize signal detection and improve imaging resolution. Excited light can generate sinusoidal fringe patterns through the grating to irradiate the sample as shown in the left of Figure 7d. SIM usually only needs to capture nine frames of image, and the time resolution is much higher. In addition, excitation light intensity is also relatively low, which is suitable for living cells. However, as SIM is limited by the imaging principle, the lateral resolution can only reach about 150 nanometers, which means that although SIM has the advantage of temporal resolution compared with other super-resolution imaging technologies, it is limited by the spatial resolution and cannot meet the detection requirements of exosomes. In 2005, Gustafsson achieved a transverse resolution of 50 nm using Saturated Structured Illumination Microscopy (SSIM, Northrop Grumman PolyScientific, Charlotte, NC, US), but at the cost of severe light damage and reduced imaging speed [126]. Therefore, in recent years, researchers have tried to improve the spatial resolution of SIM while retaining the advantages of live-cell imaging.

At present, the two best-optimized SIM are patterned activation nonlinear SIM (PANL-SIM) and Glazing Incidence SIM (GI-SIM). However, the resolution of both is better than 100 nm and cannot reach 50 nm. In 2015, Li et al. successfully observed images for F-actin in living COS-7 cells at the spatial resolution of 62 nm by PANL-SIM [127]. In recent years, researchers have tried to optimize algorithms to expand SIM resolution. In 2021, Boland et al. used a deep learning model to enlarge images and proposed a method to

reconstruct a 3D SIM image stack to increase the axial resolution of SIM by two times [128]. In 2022, He et al. introduced deep image prior (DIP) during the process of post-processing to design an untrained convolutional network to recover high-frequency information lost in SIM, which successfully achieved a 1.4-fold increase in horizontal resolution [129]. In the same year, Butola et al. proposed a new algorithm that eliminated the requirement of illumination peak clarity and an understanding of illumination patterns, making the instrument simple and flexible to be used with various micro-objectives, achieving an increase in resolution of 2.6 to 3.4 times [130]. Due to the limitation of resolution, SIM is rarely used in exosome studies. In 2019, Choi et al. revealed the molecular morphology of a single EV, which is expected to be used in the exploration of cancer cell EV by combining with nanoflow cytometry [124]. It is believed that SIM technology will be widely used in exosome research after breaking through the limitation of spatial resolution.

The super-resolution imaging techniques have broken through the optical diffraction limit and been successfully applied to live-cell imaging. Based on the above description, we believe that SMLM has more advantages in exosome-related imaging research from the perspective of fluorescent probe requirements, imaging spatiotemporal resolution, and the advantages of live-cell imaging. Especially, the imaging resolution of SMLM could meet the requirement for observing the diameters of exosomes, so it is widely popular in exosome imaging research in live cells. STED technology has no special requirements for fluorescent probes, and the imaging resolution also meets the requirement for observing the diameters of exosomes, but the photodamage decreases the activity of live cells because of high power loss. As a result, it is not suitable for cells *in vivo*. Thus, it is urgent for STED to develop new fluorescent probes that are resistant to bleaching or low-loss optical thresholds. SIM technology with universal probes has superior imaging temporal resolution compared with the other two technologies. Due to the limitation of imaging principles, the imaging resolution cannot meet the requirement for observing exosomes at present. Some researchers found that nonlinear SIM may improve the resolution of traditional technology, which is good for exosomes. Above all, SMLM is currently the most effective super-resolution imaging technique for exosome research, and STED or SIM has also been optimized. It is promising for super-resolution imaging technology to explore more detailed biomedical issues such as subcellular structures and functional mechanisms with the advancement of various fields.

#### 4. Summarize the Outlook

With developments in science and technology, optical technology has become the main means to explore exosome biogenesis and mechanisms of action, especially super-resolution imaging technology. It not only breaks through the diffraction limitation but also realizes three-color and multicolor imaging. It greatly combines the advantages of conventional characterization techniques and facilitates various biomedical studies based on exosomes, such as early diagnosis and typing of tumors. SIM and STED may limit the further study and application of exosomes due to photobleaching, phototoxicity, and a lack of resolution. Both algorithm optimization and the development of fluorescent probes have promoted the optimization of both, especially the development of nonlinear SIM technology, which promotes its application in exosomes. In contrast, SMLM research on exosomes has a wide range of application prospects. For example, the STORM technology can clearly and intuitively analyze the three-dimensional morphology of exosomes and functional information inside and outside cells with the advantages of super-resolution and rapid and real-time analysis. The results of basic research can lead to more medical applications. Chen Chen's team has set a good example for us. At present, researchers are also actively developing various methods to improve super-resolution imaging technology to facilitate precision medicine about exosomes.

In the future, we can expect not only the development of various characterization techniques but also the combination of exosome characterization techniques with machine learning to greatly shorten the image reconstruction time and expand the possible

directions of scientific technology and biomedical applications. In addition, nanoscale characterization imaging analysis provides a new observation for the structure and function analysis of exosomes and accelerates the process of basic research on exosomes. It objectively and systematically reveals the information exchange mechanism and interaction effect of exosome-based cell biology. We hope that the related research on exosomes can broaden our horizon for the treatment of major diseases and contribute to the solution of human health problems.

**Funding:** This research was funded by the National Natural Science Foundation of China grant number No. 62275125 and 62227818, the Fundamental Research Funds for the Central Universities (grant No. 30922010313), Shenzhen Sami Medical Center High-level Clinical Research Voyage Team Project (grant number SSMC-2024-TB5).

**Conflicts of Interest:** The authors declare no conflict of interest.

## References

1. Wan, J.C.M.; Massie, C.; Garcia-Corbacho, J.; Mouliere, F.; Brenton, J.D.; Caldas, C.; Pacey, S.; Baird, R.; Rosenfeld, N. Liquid biopsies come of age: Towards implementation of circulating tumour DNA. *Nat. Rev. Cancer* **2017**, *17*, 223–238. [[CrossRef](#)]
2. Alix-Panabières, C.; Pantel, K. Circulating tumor cells: Liquid biopsy of cancer. *Clin. Chem.* **2013**, *59*, 110–118. [[CrossRef](#)] [[PubMed](#)]
3. Guo, L.C.; He, B. Extracellular vesicles and their diagnostic and prognostic potential in cancer. *Transl. Cancer Res.* **2017**, *6*, 599–612. [[CrossRef](#)]
4. Huang, T.; Deng, C.X. Current Progresses of Exosomes as Cancer Diagnostic and Prognostic Biomarkers. *Int. J. Biol. Sci.* **2019**, *15*, 1–11. [[CrossRef](#)] [[PubMed](#)]
5. Im, E.J.; Lee, C.H.; Moon, P.G.; Rangaswamy, G.G.; Lee, B.; Lee, J.M.; Lee, J.C.; Jee, J.G.; Bae, J.S.; Kwon, T.K.; et al. Sulfoxazole inhibits the secretion of small extracellular vesicles by targeting the endothelin receptor A. *Nat. Commun.* **2019**, *10*, 1387. [[CrossRef](#)]
6. Junker, K.; Heinzelmann, J.; Beckham, C.; Ochiya, T.; Jenster, G. Extracellular Vesicles and Their Role in Urologic Malignancies. *Eur. Urol.* **2016**, *70*, 323–331. [[CrossRef](#)]
7. Akers, J.C.; Ramakrishnan, V.; Kim, R.; Phillips, S.; Kaimal, V.; Mao, Y.; Hua, W.; Yang, I.; Fu, C.C.; Nolan, J.; et al. miRNA contents of cerebrospinal fluid extracellular vesicles in glioblastoma patients. *J. Neuro-Oncol.* **2015**, *123*, 205–216. [[CrossRef](#)] [[PubMed](#)]
8. Minciacchi, V.R.; Freeman, M.R.; Di Vizio, D. Extracellular vesicles in cancer: Exosomes, microvesicles and the emerging role of large oncosomes. *Semin. Cell Dev. Biol.* **2015**, *40*, 41–51. [[CrossRef](#)]
9. Ciardiello, C.; Cavallini, L.; Spinelli, C.; Yang, J.; Reis-Sobreiro, M.; de Candia, P.; Minciacchi, V.R.; Di Vizio, D. Focus on Extracellular Vesicles: New Frontiers of Cell-to-Cell Communication in Cancer. *Int. J. Mol. Sci.* **2016**, *17*, 175. [[CrossRef](#)]
10. Liu, J.; Ren, L.; Li, S.; Li, W.; Zheng, X.; Yang, Y.; Fu, W.; Yi, J.; Wang, J.; Du, G. The biology, function, and applications of exosomes in cancer. *Acta Pharm. Sin. B* **2021**, *11*, 2783–2797. [[CrossRef](#)]
11. Duijvesz, D.; Luider, T.; Bangma, C.H.; Jenster, G. Exosomes as biomarker treasure chests for prostate cancer. *Eur. Urol.* **2011**, *59*, 823–831. [[CrossRef](#)] [[PubMed](#)]
12. Kimiz-Gebologlu, I.; Oncel, S.S. Exosomes: Large-scale production, isolation, drug loading efficiency, and biodistribution and uptake. *J. Control. Release* **2022**, *347*, 533–543. [[CrossRef](#)] [[PubMed](#)]
13. Andreu, Z.; Yáñez-Mó, M. Tetraspanins in extracellular vesicle formation and function. *Front. Immunol.* **2014**, *5*, 442. [[CrossRef](#)] [[PubMed](#)]
14. Berditchevski, F.; Odintsova, E. Tetraspanins as regulators of protein trafficking. *Traffic* **2007**, *8*, 89–96. [[CrossRef](#)] [[PubMed](#)]
15. Rezaie, J.; Akbari, A.; Rahbarghazi, R. Inhibition of extracellular vesicle biogenesis in tumor cells: A possible way to reduce tumorigenesis. *Cell Biochem. Funct.* **2022**, *40*, 248–262. [[CrossRef](#)]
16. Boucheix, C.; Rubinstein, E. Tetraspanins. *Cell. Mol. Life Sci.* **2001**, *58*, 1189–1205. [[CrossRef](#)]
17. He, C.; Zheng, S.; Luo, Y.; Wang, B. Exosome Theranostics: Biology and Translational Medicine. *Theranostics* **2018**, *8*, 237–255. [[CrossRef](#)]
18. He, M.; Crow, J.; Roth, M.; Zeng, Y.; Godwin, A.K. Integrated immunoisolation and protein analysis of circulating exosomes using microfluidic technology. *Lab Chip* **2014**, *14*, 3773–3780. [[CrossRef](#)]
19. Nikishin, I.; Dulimov, R.; Skryabin, G.; Galetsky, S.; Tchekina, E.; Bagrov, D. ScanEV—A neural network-based tool for the automated detection of extracellular vesicles in TEM images. *Micron* **2021**, *145*, 103044. [[CrossRef](#)]
20. Kahlert, C.; Kalluri, R. Exosomes in tumor microenvironment influence cancer progression and metastasis. *J. Mol. Med.* **2013**, *91*, 431–437. [[CrossRef](#)]
21. Wang, X.; Huang, J.; Chen, W.; Li, G.; Li, Z.; Lei, J. The updated role of exosomal proteins in the diagnosis, prognosis, and treatment of cancer. *Exp. Mol. Med.* **2022**, *54*, 1390–1400. [[CrossRef](#)]
22. Hoshino, A.; Kim, H.S.; Bojmar, L.; Gyan, K.E.; Cioffi, M.; Hernandez, J.; Zambirinis, C.P.; Rodrigues, G.; Molina, H.; Heissel, S.; et al. Extracellular Vesicle and Particle Biomarkers Define Multiple Human Cancers. *Cell* **2020**, *182*, 1044–1061. [[CrossRef](#)]



23. Risha, Y.; Minic, Z.; Ghobadloo, S.M.; Berezovski, M.V. The proteomic analysis of breast cell line exosomes reveals disease patterns and potential biomarkers. *Sci. Rep.* **2020**, *10*, 13572. [[CrossRef](#)]
24. Haraszti, R.A.; Didiot, M.C.; Sapp, E.; Leszyk, J.; Shaffer, S.A.; Rockwell, H.E.; Gao, F.; Narain, N.R.; DiFiglia, M.; Kiebish, M.A.; et al. High-resolution proteomic and lipidomic analysis of exosomes and microvesicles from different cell sources. *J. Extracell. Vesicles* **2016**, *5*, 32570. [[CrossRef](#)] [[PubMed](#)]
25. Zaborowski, M.P.; Balaj, L.; Breakefield, X.O.; Lai, C.P. Extracellular Vesicles: Composition, Biological Relevance, and Methods of Study. *Bioscience* **2015**, *65*, 783–797. [[CrossRef](#)] [[PubMed](#)]
26. Yang, B.; Chen, Y.; Shi, J. Exosome Biochemistry and Advanced Nanotechnology for Next-Generation Theranostic Platforms. *Adv. Mater.* **2019**, *31*, e1802896. [[CrossRef](#)] [[PubMed](#)]
27. Yu, D.; Li, Y.; Wang, M.; Gu, J.; Xu, W.; Cai, H.; Fang, X.; Zhang, X. Exosomes as a new frontier of cancer liquid biopsy. *Mol. Cancer* **2022**, *21*, 56. [[CrossRef](#)] [[PubMed](#)]
28. Hsu, M.T.; Wang, Y.K.; Tseng, Y.J. Exosomal Proteins and Lipids as Potential Biomarkers for Lung Cancer Diagnosis, Prognosis, and Treatment. *Cancers* **2022**, *14*, 732. [[CrossRef](#)]
29. Lee, Y.R.; Kim, G.; Tak, W.Y.; Jang, S.Y.; Kweon, Y.O.; Park, J.G.; Lee, H.W.; Han, Y.S.; Chun, J.M.; Park, S.Y.; et al. Circulating exosomal noncoding RNAs as prognostic biomarkers in human hepatocellular carcinoma. *Int. J. Cancer* **2019**, *144*, 1444–1452. [[CrossRef](#)]
30. Zhu, L.; Sun, H.T.; Wang, S.; Huang, S.L.; Zheng, Y.; Wang, C.Q.; Hu, B.Y.; Qin, W.; Zou, T.T.; Fu, Y.; et al. Isolation and characterization of exosomes for cancer research. *J. Hematol. Oncol.* **2020**, *13*, 152. [[CrossRef](#)]
31. Liu, Y.; Zhou, Z.; Wang, F.; Kewes, G.; Wen, S.; Burger, S.; Ebrahimi Wakiani, M.; Xi, P.; Yang, J.; Yang, X.; et al. Axial localization and tracking of self-interference nanoparticles by lateral point spread functions. *Nat. Commun.* **2021**, *12*, 2019. [[CrossRef](#)] [[PubMed](#)]
32. Wu, H.J.; Huang, C.L.; Wang, L.W.; Li, Q.H.; Li, Y.J.; Zhang, L.H.; Zhu, D.W. Folate-targeted co-delivery polymersomes for efficient photo-chemo-antiangiogenic therapy against breast cancer and in vivo evaluation via OCTA\_NIRF dual-modal imaging-3. *Chin. Chem. Lett.* **2022**, *33*, 5035–5041. [[CrossRef](#)]
33. Filipe, V.; Hawe, A.; Jiskoot, W. Critical evaluation of Nanoparticle Tracking Analysis (NTA) by NanoSight for the measurement of nanoparticles and protein aggregates. *Pharm. Res.* **2010**, *27*, 796–810. [[CrossRef](#)] [[PubMed](#)]
34. Libregts, S.; Arkesteijn, G.J.A.; Németh, A.; Nolte-'t Hoen, E.N.M.; Wauben, M.H.M. Flow cytometric analysis of extracellular vesicle subsets in plasma: Impact of swarm by particles of non-interest. *J. Thromb. Haemost.* **2018**, *16*, 1423–1436. [[CrossRef](#)] [[PubMed](#)]
35. Arraud, N.; Linares, R.; Tan, S.; Gounou, C.; Pasquet, J.M.; Mornet, S.; Brisson, A.R. Extracellular vesicles from blood plasma: Determination of their morphology, size, phenotype and concentration. *J. Thromb. Haemost.* **2014**, *12*, 614–627. [[CrossRef](#)] [[PubMed](#)]
36. Lai, J.J.; Chau, Z.L.; Chen, S.Y.; Hill, J.J.; Korpany, K.V.; Liang, N.W.; Lin, L.H.; Lin, Y.H.; Liu, J.K.; Liu, Y.C.; et al. Exosome Processing and Characterization Approaches for Research and Technology Development. *Adv. Sci.* **2022**, *9*, e2103222. [[CrossRef](#)]
37. Mashouri, L.; Yousefi, H.; Aref, A.R.; Ahadi, A.M.; Molaei, F.; Alahari, S.K. Exosomes: Composition, biogenesis, and mechanisms in cancer metastasis and drug resistance. *Mol. Cancer* **2019**, *18*, 75. [[CrossRef](#)]
38. Dai, J.; Su, Y.; Zhong, S.; Cong, L.; Liu, B.; Yang, J.; Tao, Y.; He, Z.; Chen, C.; Jiang, Y. Exosomes: Key players in cancer and potential therapeutic strategy. *Signal Transduct. Target. Ther.* **2020**, *5*, 145. [[CrossRef](#)]
39. Jiang, C.; Zhang, N.; Hu, X.; Wang, H. Tumor-associated exosomes promote lung cancer metastasis through multiple mechanisms. *Mol. Cancer* **2021**, *20*, 117. [[CrossRef](#)]
40. Zhao, S.; Mi, Y.; Guan, B.; Zheng, B.; Wei, P.; Gu, Y.; Zhang, Z.; Cai, S.; Xu, Y.; Li, X.; et al. Tumor-derived exosomal miR-934 induces macrophage M2 polarization to promote liver metastasis of colorectal cancer. *J. Hematol. Oncol.* **2020**, *13*, 156. [[CrossRef](#)]
41. Zhang, L.; Yu, D. Exosomes in cancer development, metastasis, and immunity. *Biochim. Biophys. (BBA) Acta Rev. Cancer* **2019**, *1871*, 455–468. [[CrossRef](#)] [[PubMed](#)]
42. Hartjes, T.A.; Mytnyk, S.; Jenster, G.W.; van Steijn, V.; van Royen, M.E. Extracellular Vesicle Quantification and Characterization: Common Methods and Emerging Approaches. *Bioengineering* **2019**, *6*, 7. [[CrossRef](#)] [[PubMed](#)]
43. Maas, S.L.; De Vrij, J.; Broekman, M.L. Quantification and size-profiling of extracellular vesicles using tunable resistive pulse sensing. *J. Vis. Exp.* **2014**, *92*, e51623. [[CrossRef](#)]
44. Maas, S.L.; Broekman, M.L.; de Vrij, J. Tunable Resistive Pulse Sensing for the Characterization of Extracellular Vesicles. *Methods Mol. Biol.* **2017**, *1545*, 21–33. [[CrossRef](#)] [[PubMed](#)]
45. Durak-Kozica, M.; Baster, Z.; Kubat, K.; Stępień, E. 3D visualization of extracellular vesicle uptake by endothelial cells. *Cell. Mol. Biol. Lett.* **2018**, *23*, 57. [[CrossRef](#)] [[PubMed](#)]
46. Vogel, R.; Pal, A.K.; Jambhrunkar, S.; Patel, P.; Thakur, S.S.; Reátegui, E.; Parekh, H.S.; Saá, P.; Stassinopoulos, A.; Broom, M.F. High-Resolution Single Particle Zeta Potential Characterisation of Biological Nanoparticles using Tunable Resistive Pulse Sensing. *Sci. Rep.* **2017**, *7*, 17479. [[CrossRef](#)] [[PubMed](#)]
47. Malenica, M.; Vukomanović, M.; Kurtjak, M.; Masciotti, V.; Dal Zilio, S.; Greco, S.; Lazzarino, M.; Krušić, V.; Perčić, M.; Jelovica Badovinac, I.; et al. Perspectives of Microscopy Methods for Morphology Characterisation of Extracellular Vesicles from Human Biofluids. *Biomedicines* **2021**, *9*, 603. [[CrossRef](#)]

48. McNamara, R.P.; Zhou, Y.; Eason, A.B.; Landis, J.T.; Chambers, M.G.; Willcox, S.; Peterson, T.A.; Schouest, B.; Maness, N.J.; MacLean, A.G.; et al. Imaging of surface microdomains on individual extracellular vesicles in 3-D. *J. Extracell. Vesicles* **2022**, *11*, e12191. [[CrossRef](#)]
49. Fakhredini, F.; Mansouri, E.; Mard, S.A.; Valizadeh Gorji, A.; Rashno, M.; Orazizadeh, M. Effects of Exosomes Derived from Kidney Tubular Cells on Diabetic Nephropathy in Rats. *Cell J.* **2022**, *24*, 28–35. [[CrossRef](#)]
50. Conde-Vancells, J.; Rodriguez-Suarez, E.; Embade, N.; Gil, D.; Matthiesen, R.; Valle, M.; Elortza, F.; Lu, S.C.; Mato, J.M.; Falcon-Perez, J.M. Characterization and comprehensive proteome profiling of exosomes secreted by hepatocytes. *J. Proteome Res.* **2008**, *7*, 5157–5166. [[CrossRef](#)]
51. Jeong, D.; Kim, M.J.; Park, Y.; Chung, J.; Kweon, H.S.; Kang, N.G.; Hwang, S.J.; Youn, S.H.; Hwang, B.K.; Kim, D. Visualizing extracellular vesicle biogenesis in gram-positive bacteria using super-resolution microscopy. *BMC Biol.* **2022**, *20*, 270. [[CrossRef](#)] [[PubMed](#)]
52. Zabeo, D.; Cvjetkovic, A.; Lässer, C.; Schorb, M.; Lötvall, J.; Höög, J.L. Exosomes purified from a single cell type have diverse morphology. *J. Extracell. Vesicles* **2017**, *6*, 1329476. [[CrossRef](#)] [[PubMed](#)]
53. Gardiner, C.; Di Vizio, D.; Sahoo, S.; Théry, C.; Witwer, K.W.; Wauben, M.; Hill, A.F. Techniques used for the isolation and characterization of extracellular vesicles: Results of a worldwide survey. *J. Extracell. Vesicles* **2016**, *5*, 32945. [[CrossRef](#)] [[PubMed](#)]
54. Issman, L.; Brenner, B.; Talmon, Y.; Aharon, A. Cryogenic transmission electron microscopy nanostructural study of shed microparticles. *PLoS ONE* **2013**, *8*, e83680. [[CrossRef](#)] [[PubMed](#)]
55. Jung, M.K.; Mun, J.Y. Sample Preparation and Imaging of Exosomes by Transmission Electron Microscopy. *J. Vis. Exp.* **2018**, *131*, e56482. [[CrossRef](#)]
56. Božič, D.; Hočevár, M.; Kisovec, M.; Pajnič, M.; Pađen, L.; Jeran, M.; Bedina Zavec, A.; Podobnik, M.; Kogej, K.; Iglič, A.; et al. Stability of Erythrocyte-Derived Nanovesicles Assessed by Light Scattering and Electron Microscopy. *Int. J. Mol. Sci.* **2021**, *22*, 12772. [[CrossRef](#)] [[PubMed](#)]
57. Sokolova, V.; Ludwig, A.K.; Hornung, S.; Rotan, O.; Horn, P.A.; Epple, M.; Giebel, B. Characterisation of exosomes derived from human cells by nanoparticle tracking analysis and scanning electron microscopy. *Colloids Surf. B Biointerfaces* **2011**, *87*, 146–150. [[CrossRef](#)]
58. Cizmar, P.; Yuana, Y. Detection and Characterization of Extracellular Vesicles by Transmission and Cryo-Transmission Electron Microscopy. *Methods Mol. Biol.* **2017**, *1660*, 221–232. [[CrossRef](#)]
59. Liu, Z.; Xue, H.; Chen, Q.; Yang, G. A method for extraction of exosomes from breast tumour cells and characterisation by transmission electron microscopy. *J. Microsc.* **2023**, *292*, 117–122. [[CrossRef](#)]
60. Park, Y.H.; Shin, H.W.; Jung, A.R.; Kwon, O.S.; Choi, Y.J.; Park, J.; Lee, J.Y. Prostate-specific extracellular vesicles as a novel biomarker in human prostate cancer. *Sci. Rep.* **2016**, *6*, 30386. [[CrossRef](#)]
61. Kurtjak, M.; Kereiche, S.; Klepac, D.; Križan, H.; Perčić, M.; Krušić Alić, V.; Lavrin, T.; Lenassi, M.; Wechtersbach, K.; Kojc, N.; et al. Unveiling the Native Morphology of Extracellular Vesicles from Human Cerebrospinal Fluid by Atomic Force and Cryogenic Electron Microscopy. *Biomedicines* **2022**, *10*, 1251. [[CrossRef](#)] [[PubMed](#)]
62. Stetefeld, J.; McKenna, S.A.; Patel, T.R. Dynamic light scattering: A practical guide and applications in biomedical sciences. *Biophys. Rev.* **2016**, *8*, 409–427. [[CrossRef](#)] [[PubMed](#)]
63. Palmieri, V.; Lucchetti, D.; Gatto, I.; Maiorana, A.; Marcantoni, M.; Maulucci, G.; Papi, M.; Pola, R.; De Spirito, M.; Sgambato, A. Dynamic light scattering for the characterization and counting of extracellular vesicles: A powerful noninvasive tool. *J. Nanopart. Res.* **2014**, *16*, 2583. [[CrossRef](#)]
64. Perpetuo, L.; Ferreira, R.; Thongboonkerd, V.; Guedes, S.; Amado, F.; Vitorino, R. Urinary exosomes: Diagnostic impact with a bioinformatic approach. *Adv. Clin. Chem.* **2022**, *111*, 69–99. [[CrossRef](#)] [[PubMed](#)]
65. Gercel-Taylor, C.; Atay, S.; Tullis, R.H.; Kesimer, M.; Taylor, D.D. Nanoparticle analysis of circulating cell-derived vesicles in ovarian cancer patients. *Anal. Biochem.* **2012**, *428*, 44–53. [[CrossRef](#)] [[PubMed](#)]
66. Tajik, T.; Baghaei, K.; Moghadam, V.E.; Farrokhi, N.; Salami, S.A. Extracellular vesicles of cannabis with high CBD content induce anticancer signaling in human hepatocellular carcinoma. *Biomed. Pharmacother.* **2022**, *152*, 113209. [[CrossRef](#)]
67. Hassan, P.A.; Rana, S.; Verma, G. Making sense of Brownian motion: Colloid characterization by dynamic light scattering. *Langmuir* **2015**, *31*, 3–12. [[CrossRef](#)]
68. Lawrie, A.S.; Albany, A.; Cardigan, R.A.; Mackie, I.J.; Harrison, P. Microparticle sizing by dynamic light scattering in fresh-frozen plasma. *Vox Sang.* **2009**, *96*, 206–212. [[CrossRef](#)]
69. Szatanek, R.; Baj-Krzyworzeka, M.; Zimoch, J.; Lekka, M.; Siedlar, M.; Baran, J. The Methods of Choice for Extracellular Vesicles (EVs) Characterization. *Int. J. Mol. Sci.* **2017**, *18*, 1153. [[CrossRef](#)]
70. Cho, S.; Yi, J.; Kwon, Y.; Kang, H.; Han, C.; Park, J. Multifluorescence Single Extracellular Vesicle Analysis by Time-Sequential Illumination and Tracking. *ACS Nano* **2021**, *15*, 11753–11761. [[CrossRef](#)]
71. Vestad, B.; Llorente, A.; Neurauter, A.; Phuyal, S.; Kierulf, B.; Kierulf, P.; Skotland, T.; Sandvig, K.; Haug, K.B.F.; Øvstebø, R. Size and concentration analyses of extracellular vesicles by nanoparticle tracking analysis: A variation study. *J. Extracell. Vesicles* **2017**, *6*, 1344087. [[CrossRef](#)] [[PubMed](#)]
72. Dragovic, R.A.; Gardiner, C.; Brooks, A.S.; Tannetta, D.S.; Ferguson, D.J.; Hole, P.; Carr, B.; Redman, C.W.; Harris, A.L.; Dobson, P.J.; et al. Sizing and phenotyping of cellular vesicles using Nanoparticle Tracking Analysis. *Nanomed. Nanotechnol. Biol. Med.* **2011**, *7*, 780–788. [[CrossRef](#)] [[PubMed](#)]

73. Gardiner, C.; Shaw, M.; Hole, P.; Smith, J.; Tannetta, D.; Redman, C.W.; Sargent, I.L. Measurement of refractive index by nanoparticle tracking analysis reveals heterogeneity in extracellular vesicles. *J. Extracell. Vesicles* **2014**, *3*, 25361. [[CrossRef](#)]
74. Saari, H.; Lisitsyna, E.; Rautaniemi, K.; Rojalín, T.; Niemi, L.; Nivaro, O.; Laaksonen, T.; Yliperttula, M.; Vuorimaa-Laukkanen, E. FLIM reveals alternative EV-mediated cellular up-take pathways of paclitaxel. *J. Control. Release* **2018**, *284*, 133–143. [[CrossRef](#)]
75. Shao, H.; Chung, J.; Balaj, L.; Charest, A.; Bigner, D.D.; Carter, B.S.; Hochberg, F.H.; Breakefield, X.O.; Weissleder, R.; Lee, H. Protein typing of circulating microvesicles allows real-time monitoring of glioblastoma therapy. *Nat. Med.* **2012**, *18*, 1835–1840. [[CrossRef](#)] [[PubMed](#)]
76. van der Pol, E.; Coumans, F.A.; Grootemaat, A.E.; Gardiner, C.; Sargent, I.L.; Harrison, P.; Sturk, A.; van Leeuwen, T.G.; Nieuwland, R. Particle size distribution of exosomes and microvesicles determined by transmission electron microscopy, flow cytometry, nanoparticle tracking analysis, and resistive pulse sensing. *J. Thromb. Haemost.* **2014**, *12*, 1182–1192. [[CrossRef](#)]
77. Hu, Y.; Tian, Y.; Di, H.; Xue, C.; Zheng, Y.; Hu, B.; Lin, Q.; Yan, X. Noninvasive Diagnosis of Nasopharyngeal Carcinoma Based on Phenotypic Profiling of Viral and Tumor Markers on Plasma Extracellular Vesicles. *Anal. Chem.* **2022**, *94*, 9740–9749. [[CrossRef](#)]
78. Liu, H.S.; Tian, Y.; Xue, C.F.; Niu, Q.; Chen, C.; Yan, X.M. Analysis of extracellular vesicle DNA at the single-vesicle level by nano-flow cytometry. *J. Extracell. Vesicles* **2022**, *11*, e12206. [[CrossRef](#)]
79. Lees, R.; Tempest, R.; Law, A.; Aubert, D.; Davies, O.G.; Williams, S.; Peake, N.; Peacock, B. Single Extracellular Vesicle Transmembrane Protein Characterization by Nano-Flow Cytometry. *J. Vis. Exp.* **2022**, *185*, e64020. [[CrossRef](#)]
80. Ricklefs, F.L.; Maire, C.L.; Reimer, R.; Dührsen, L.; Kolbe, K.; Holz, M.; Schneider, E.; Rissiek, A.; Babayan, A.; Hille, C.; et al. Imaging flow cytometry facilitates multiparametric characterization of extracellular vesicles in malignant brain tumours. *J. Extracell. Vesicles* **2019**, *8*, 1588555. [[CrossRef](#)]
81. Aibaidula, A.Z.; Fain, C.E.; Garcia, L.C.; Wier, A.; Bouchal, S.M.; Bauman, M.M.; Jung, M.Y.; Sarkaria, J.N.; Johnson, A.J.; Parney, I.F. Spectral flow cytometry identifies distinct nonneoplastic plasma extracellular vesicle phenotype in glioblastoma patients. *Neuro-Oncol. Adv.* **2023**, *5*, vdad082. [[CrossRef](#)]
82. Betzig, E.; Patterson, G.H.; Sougrat, R.; Lindwasser, O.W.; Olenych, S.; Bonifacino, J.S.; Davidson, M.W.; Lippincott-Schwartz, J.; Hess, H.F. Imaging intracellular fluorescent proteins at nanometer resolution. *Science* **2006**, *313*, 1642–1645. [[CrossRef](#)] [[PubMed](#)]
83. Rust, M.J.; Bates, M.; Zhuang, X. Sub-diffraction-limit imaging by stochastic optical reconstruction microscopy (STORM). *Nat. Methods* **2006**, *3*, 793–795. [[CrossRef](#)] [[PubMed](#)]
84. van de Linde, S.; Löschberger, A.; Klein, T.; Heidebreder, M.; Wolter, S.; Heilemann, M.; Sauer, M. Direct stochastic optical reconstruction microscopy with standard fluorescent probes. *Nat. Protoc.* **2011**, *6*, 991–1009. [[CrossRef](#)] [[PubMed](#)]
85. Jones, S.A.; Shim, S.H.; He, J.; Zhuang, X. Fast, three-dimensional super-resolution imaging of live cells. *Nat. Methods* **2011**, *8*, 499–508. [[CrossRef](#)] [[PubMed](#)]
86. Zhu, L.; Zhang, W.; Elnatan, D.; Huang, B. Faster STORM using compressed sensing. *Nat. Methods* **2012**, *9*, 721–723. [[CrossRef](#)]
87. Chen, B.; Gong, W.; Yang, Z.; Pan, W.; Verwilt, P.; Shin, J.; Yan, W.; Liu, L.; Qu, J.; Kim, J.S. STORM imaging of mitochondrial dynamics using a vicinal-dithiol-proteins-targeted probe. *Biomaterials* **2020**, *243*, 119938. [[CrossRef](#)]
88. Ouyang, W.; Aristov, A.; Lelek, M.; Hao, X.; Zimmer, C. Deep learning massively accelerates super-resolution localization microscopy. *Nat. Biotechnol.* **2018**, *36*, 460–468. [[CrossRef](#)]
89. Helmerich, D.A.; Beliu, G.; Taban, D.; Meub, M.; Streit, M.; Kuhlemann, A.; Doose, S.; Sauer, M. Photoswitching fingerprint analysis bypasses the 10-nm resolution barrier. *Nat. Methods* **2022**, *19*, 986–994. [[CrossRef](#)]
90. Dechantsreiter, S.; Ambrose, A.R.; Worboys, J.D.; Lim, J.M.E.; Liu, S.; Shah, R.; Montero, M.A.; Quinn, A.M.; Hussell, T.; Tannahill, G.M.; et al. Heterogeneity in extracellular vesicle secretion by single human macrophages revealed by super-resolution microscopy. *J. Extracell. Vesicles* **2022**, *11*, e12215. [[CrossRef](#)]
91. Chen, C.; Zong, S.; Wang, Z.; Lu, J.; Zhu, D.; Zhang, Y.; Cui, Y. Imaging and Intracellular Tracking of Cancer-Derived Exosomes Using Single-Molecule Localization-Based Super-Resolution Microscope. *ACS Appl. Mater. Interfaces* **2016**, *8*, 25825–25833. [[CrossRef](#)] [[PubMed](#)]
92. Shim, S.H.; Xia, C.; Zhong, G.; Babcock, H.P.; Vaughan, J.C.; Huang, B.; Wang, X.; Xu, C.; Bi, G.Q.; Zhuang, X. Super-resolution fluorescence imaging of organelles in live cells with photoswitchable membrane probes. *Proc. Natl. Acad. Sci. USA* **2012**, *109*, 13978–13983. [[CrossRef](#)]
93. Zong, S.; Zong, J.; Chen, C.; Jiang, X.; Zhang, Y.; Wang, Z.; Cui, Y. Single molecule localization imaging of exosomes using blinking silicon quantum dots. *Nanotechnology* **2018**, *29*, 065705. [[CrossRef](#)] [[PubMed](#)]
94. Chen, C.; Zong, S.; Wang, Z.; Lu, J.; Zhu, D.; Zhang, Y.; Zhang, R.; Cui, Y. Visualization and intracellular dynamic tracking of exosomes and exosomal miRNAs using single molecule localization microscopy. *Nanoscale* **2018**, *10*, 5154–5162. [[CrossRef](#)]
95. Mondal, A.; Ashiq, K.A.; Phulpagar, P.; Singh, D.K.; Shiras, A. Effective Visualization and Easy Tracking of Extracellular Vesicles in Glioma Cells. *Biol. Proced. Online* **2019**, *21*, 4. [[CrossRef](#)]
96. Saftics, A.; Abuelreich, S.; Romano, E.; Ghaeli, I.; Jiang, N.; Spanos, M.; Lennon, K.M.; Singh, G.; Das, S.; Van Keuren-Jensen, K.; et al. Single Extracellular Vesicle Nanoscopy. *J. Extracell. Vesicles* **2023**, *12*, e12346. [[CrossRef](#)] [[PubMed](#)]
97. Oleksiuk, O.; Abba, M.; Tezcan, K.C.; Schaufler, W.; Bestvater, F.; Patil, N.; Birk, U.; Hafner, M.; Altevogt, P.; Cremer, C.; et al. Single-Molecule Localization Microscopy allows for the analysis of cancer metastasis-specific miRNA distribution on the nanoscale. *Oncotarget* **2015**, *6*, 44745–44757. [[CrossRef](#)]
98. Wei, J.; Zhang, S.; Yuan, J.; Wang, Z.; Zong, S.; Cui, Y. Nanoscale imaging of tumor cell exosomes by expansion single molecule localization microscopy (ExSMLM). *Talanta* **2023**, *261*, 124641. [[CrossRef](#)]

99. Lennon, K.M.; Wakefield, D.L.; Maddox, A.L.; Brehove, M.S.; Willner, A.N.; Garcia-Mansfield, K.; Meechoovet, B.; Reiman, R.; Hutchins, E.; Miller, M.M.; et al. Single molecule characterization of individual extracellular vesicles from pancreatic cancer. *J. Extracell. Vesicles* **2019**, *8*, 1685634. [[CrossRef](#)]
100. Wei, Y.X.; Han, J.H.; Shen, H.M.; Wang, Y.Y.; Qi, M.; Wang, L.; Li, J. Highly sensitive fluorescent detection of EDIL3 overexpressed exosomes for the diagnosis of triple-negative breast cancer. *Nanotechnology* **2022**, *33*, 425204. [[CrossRef](#)]
101. Jungmann, R.; Avendaño, M.S.; Woehrstein, J.B.; Dai, M.; Shih, W.M.; Yin, P. Multiplexed 3D cellular super-resolution imaging with DNA-PAINT and Exchange-PAINT. *Nat. Methods* **2014**, *11*, 313–318. [[CrossRef](#)]
102. Tholen, M.M.E.; Tas, R.P.; Wang, Y.; Albertazzi, L. Beyond DNA: New probes for PAINT super-resolution microscopy. *Chem. Commun.* **2023**, *59*, 8332–8342. [[CrossRef](#)] [[PubMed](#)]
103. Chen, C.; Zong, S.; Liu, Y.; Wang, Z.; Zhang, Y.; Chen, B.; Cui, Y. Profiling of Exosomal Biomarkers for Accurate Cancer Identification: Combining DNA-PAINT with Machine-Learning-Based Classification. *Small* **2019**, *15*, e1901014. [[CrossRef](#)] [[PubMed](#)]
104. Liu, D.A.; Tao, K.; Wu, B.; Yu, Z.; Szczepaniak, M.; Rames, M.; Yang, C.; Svitkina, T.; Zhu, Y.; Xu, F.; et al. A phosphoinositide switch mediates exocyst recruitment to multivesicular endosomes for exosome secretion. *Nat. Commun.* **2023**, *14*, 6883. [[CrossRef](#)] [[PubMed](#)]
105. Auer, A.; Strauss, M.T.; Schlichthaerle, T.; Jungmann, R. Fast, Background-Free DNA-PAINT Imaging Using FRET-Based Probes. *Nano Lett.* **2017**, *17*, 6428–6434. [[CrossRef](#)] [[PubMed](#)]
106. Zhu, M.; Zhang, L.; Jin, L.; Chen, J.; Zhang, Y.; Xu, Y. DNA-PAINT Imaging Accelerated by Machine Learning. *Front. Chem.* **2022**, *10*, 864701. [[CrossRef](#)] [[PubMed](#)]
107. van Wee, R.; Filius, M.; Joo, C. Completing the canvas: Advances and challenges for DNA-PAINT super-resolution imaging. *Trends Biochem. Sci.* **2021**, *46*, 918–930. [[CrossRef](#)]
108. McEvoy, A.L.; Greenfield, D.; Bates, M.; Liphardt, J. Q&A: Single-molecule localization microscopy for biological imaging. *BMC Biol.* **2010**, *8*, 106. [[CrossRef](#)]
109. Nieves, D.J.; Gaus, K.; Baker, M.A.B. DNA-Based Super-Resolution Microscopy: DNA-PAINT. *Genes* **2018**, *9*, 621. [[CrossRef](#)]
110. Strauss, S.; Jungmann, R. Up to 100-fold speed-up and multiplexing in optimized DNA-PAINT. *Nat. Methods* **2020**, *17*, 789–791. [[CrossRef](#)]
111. Li, W.; Li, C.; Zhou, T.; Liu, X.; Li, X.; Chen, D. Role of exosomal proteins in cancer diagnosis. *Mol. Cancer* **2017**, *16*, 145. [[CrossRef](#)] [[PubMed](#)]
112. Bai, S.; Hou, W.; Yao, Y.; Meng, J.; Wei, Y.; Hu, F.; Hu, X.; Wu, J.; Zhang, N.; Xu, R.; et al. Exocyst controls exosome biogenesis via Rab11a. *Mol. Ther. Nucleic Acids* **2022**, *27*, 535–546. [[CrossRef](#)]
113. Hell, S.W.; Wichmann, J. Breaking the diffraction resolution limit by stimulated emission: Stimulated-emission-depletion fluorescence microscopy. *Opt. Lett.* **1994**, *19*, 780–782. [[CrossRef](#)] [[PubMed](#)]
114. Butkevich, A.N.; Mitronova, G.Y.; Sidenstein, S.C.; Klocke, J.L.; Kamin, D.; Meineke, D.N.; D'Este, E.; Kraemer, P.T.; Danzl, J.G.; Belov, V.N.; et al. Fluorescent Rhodamines and Fluorogenic Carbopyronines for Super-Resolution STED Microscopy in Living Cells. *Angew. Chem. Int. Ed.* **2016**, *55*, 3290–3294. [[CrossRef](#)]
115. Pajk, S.; Majaron, H.; Novak, M.; Kokot, B.; Štrancar, J. New coumarin- and phenoxazine-based fluorescent probes for live-cell STED nanoscopy. *Eur. Biophys. J.* **2019**, *48*, 485–490. [[CrossRef](#)]
116. Valcz, G.; Buzás, E.I.; Kittel, Á.; Krenács, T.; Visnovitz, T.; Spisák, S.; Török, G.; Homolya, L.; Zsigrai, S.; Kiszler, G.; et al. En bloc release of MVB-like small extracellular vesicle clusters by colorectal carcinoma cells. *J. Extracell. Vesicles* **2019**, *8*, 1596668. [[CrossRef](#)]
117. Yang, X.; Yang, Z.; Wu, Z.; He, Y.; Shan, C.; Chai, P.; Ma, C.; Tian, M.; Teng, J.; Jin, D.; et al. Mitochondrial dynamics quantitatively revealed by STED nanoscopy with an enhanced squaraine variant probe. *Nat. Commun.* **2020**, *11*, 3699. [[CrossRef](#)]
118. Alvelid, J.; Damenti, M.; Sgattoni, C.; Testa, I. Event-triggered STED imaging. *Nat. Methods* **2022**, *19*, 1268–1275. [[CrossRef](#)]
119. Liu, Y.; Zhou, J.; Wen, S.; Wang, F.; Wu, H.; Chen, Q.; Zuo, C.; Jin, D. On-Chip Mirror Enhanced Multiphoton Upconversion Super-Resolution Microscopy. *Nano Lett.* **2023**, *23*, 5514–5519. [[CrossRef](#)]
120. Liu, Y.; Wang, F.; Lu, H.; Fang, G.; Wen, S.; Chen, C.; Shan, X.; Xu, X.; Zhang, L.; Stenzel, M.; et al. Super-Resolution Mapping of Single Nanoparticles inside Tumor Spheroids. *Small* **2020**, *16*, e1905572. [[CrossRef](#)]
121. Huang, G.; Liu, Y.; Wang, D.; Zhu, Y.; Wen, S.; Ruan, J.; Jin, D. Upconversion nanoparticles for super-resolution quantification of single small extracellular vesicles. *eLight* **2022**, *2*, 20. [[CrossRef](#)]
122. Liu, Y.; Wen, S.; Wang, F.; Zuo, C.; Chen, C.; Zhou, J.; Jin, D. Population Control of Upconversion Energy Transfer for Stimulation Emission Depletion Nanoscopy. *Adv. Sci.* **2023**, *10*, e2205990. [[CrossRef](#)] [[PubMed](#)]
123. Sezgin, E. Super-resolution optical microscopy for studying membrane structure and dynamics. *J. Phys. Condens. Matter* **2017**, *29*, 273001. [[CrossRef](#)]
124. Choi, D.; Montermini, L.; Jeong, H.; Sharma, S.; Meehan, B.; Rak, J. Mapping Subpopulations of Cancer Cell-Derived Extracellular Vesicles and Particles by Nano-Flow Cytometry. *ACS Nano* **2019**, *13*, 10499–10511. [[CrossRef](#)] [[PubMed](#)]
125. Gustafsson, M.G. Surpassing the lateral resolution limit by a factor of two using structured illumination microscopy. *J. Microsc.* **2000**, *198*, 82–87. [[CrossRef](#)] [[PubMed](#)]
126. Gustafsson, M.G. Nonlinear structured-illumination microscopy: Wide-field fluorescence imaging with theoretically unlimited resolution. *Proc. Natl. Acad. Sci. USA* **2005**, *102*, 13081–13086. [[CrossRef](#)]

127. Li, D.; Shao, L.; Chen, B.C.; Zhang, X.; Zhang, M.; Moses, B.; Milkie, D.E.; Beach, J.R.; Hammer, J.A., 3rd; Pasham, M.; et al. ADVANCED IMAGING. Extended-resolution structured illumination imaging of endocytic and cytoskeletal dynamics. *Science* **2015**, *349*, aab3500. [[CrossRef](#)] [[PubMed](#)]
128. Boland, M.A.; Cohen, E.A.K.; Flaxman, S.R.; Neil, M.A.A. Improving axial resolution in Structured Illumination Microscopy using deep learning. *Philos. Trans. Ser. A Math. Phys. Eng. Sci.* **2021**, *379*, 20200298. [[CrossRef](#)]
129. He, Y.; Yao, Y.; He, Y.; Huang, Z.; Luo, F.; Zhang, C.; Qi, D.; Jia, T.; Wang, Z.; Sun, Z.; et al. Surpassing the resolution limitation of structured illumination microscopy by an untrained neural network. *Biomed. Opt. Express* **2023**, *14*, 106–117. [[CrossRef](#)]
130. Butola, A.; Acuna, S.; Hansen, D.H.; Agarwal, K. Scalable-resolution structured illumination microscopy. *Opt. Express* **2022**, *30*, 43752–43767. [[CrossRef](#)]

**Disclaimer/Publisher’s Note:** The statements, opinions and data contained in all publications are solely those of the individual author(s) and contributor(s) and not of MDPI and/or the editor(s). MDPI and/or the editor(s) disclaim responsibility for any injury to people or property resulting from any ideas, methods, instructions or products referred to in the content.